Impact of dust storm on phytoplankton bloom over the Arabian Sea: a case study during March 2012

Article *in* Environmental Science and Pollution Research · March 2019

DOI: 10.1007/s11356-019-04602-7

5 authors, including:

Kunal Bali
Indian Institute of Technology Delhi
3 PUBLICATIONS **5** CITATIONS
SEE PROFILE

A.K. Mishra
Jawaharlal Nehru University
27 PUBLICATIONS **299** CITATIONS
SEE PROFILE

Sachchidanand Singh
National Physical Laboratory - India
101 PUBLICATIONS **2,198** CITATIONS
SEE PROFILE

Subhash Chandra
National Physical Laboratory - India
6 PUBLICATIONS **28** CITATIONS
SEE PROFILE

Environmental Science and Pollution Research
https://doi.org/10.1007/s11356-019-04602-7

RESEARCH ARTICLE

Impact of dust storm on phytoplankton bloom over the Arabian Sea: a case study during March 2012

Kunal Bali[1,2] · Amit Kumar Mishra[3] · Sachchidanand Singh[1,4] · Subhash Chandra[1] · Yoav Lehahn[5]

Received: 19 September 2018 / Accepted: 18 February 2019

Abstract

Dust storms affect the primary productivity of the ocean by providing necessary micronutrients to the surface layer. One such dust storm during March 2012 led to a substantial reduction in visibility and enhancement in aerosol optical depth (AOD) up to ~ 0.8 (AOD increased from 0.1 to 0.9) over the Arabian Sea. We explored the possible effects and mechanisms through which this particular dust storm could impact the ocean's primary productivity (phytoplankton concentration), using satellite-borne remote sensors and reanalysis model data (2003–2016). The climatological analyses revealed anomalous March 2012 in terms of dust deposition and enhancement in phytoplankton concentration in the month of March during 2003–2016 over this region. The studied dust storm accounts for increase in the daily average surface dust deposition rate from ~ 3 to ~53 mg m^{-2} day^{-1}, which is followed by a significant enhancement in the chlorophyll-a (Chl_a) concentration (~ 2 to ~9 mg m^{-3}). We show strong association between a dust storm and an event of anomalously high biological production (with a 4-day forward lag) in the Arabian Sea. We suggest that the increase in biological production results from the superposition of two complementary processes (deposition of atmospheric nutrients and deepening of the mixed layer due to dust-induced sea surface temperature cooling) that enhance nutrient availability in the euphotic layer.

Keywords Phytoplankton bloom · Chlorophyll_a · Dust storm · Fe-fertilisation · Sea surface temperature · Arabian Sea

Introduction

Atmospheric dust is known to affect the Earth's climate system, directly through absorption and scattering of solar radiation and indirectly via modification of cloud properties (*Twomey* 1977; *Albrecht* 1989; *Lohmann and Feichter* 2005). Moreover, these dust aerosols alter the primary productivity of the oceans by deposition of iron (Fe) and other micronutrients on ocean surface (*Jickells* et al. 2005; *Han* et al. 2011; *Calil* et al. 2011) and have significant impact on ecological balance of oceanic ecosystem (*Patra* et al. 2007). The depositions from dust storms are more frequent and are mainly originating from the desert regions like the Sahara, Middle East, Southwest Asia, China, Mongolia, southwestern North America, west coast of South America, and Australia. For example, dust from East Asia and Sahara are known to reach far beyond their sources of origin and get deposited over the Pacific and the Atlantic Ocean and affect as far as North and South America (*Prospero* et al. 1987; *Goudie and Middleton* 2001).

These atmospheric dust aerosols are responsible for supplying micronutrients to open ocean regions (*Fung* et al. 2000; *Sarthou* et al. 2003; *Jickells* et al. 2005; *Gabric* et al. 2002), particularly the Fe to the marine ecosystems (*Duce and Tindale* 1991; *Sunda and Hunstsman* 1997; *Hutchins and Bruland* 1998). There are several important sources through which nutrients are made available to phytoplankton such as

Responsible editor: Philippe Garrigues

Electronic supplementary material The online version of this article (https://doi.org/10.1007/s11356-019-04602-7) contains supplementary material, which is available to authorized users.

✉ Sachchidanand Singh
ssingh@nplindia.org; ssinghnpl@gmail.com

[1] Environmental Sciences and Biomedical Metrology Division, CSIR-National Physical Laboratory, New Delhi 110012, India

[2] Centre for Atmospheric Sciences, Indian Institute of Technology, New Delhi 110016, India

[3] School of Environmental Sciences, Jawaharlal Nehru University, New Delhi 110067, India

[4] CSIR-National Physical Laboratory Campus, Academy of Scientific and Innovative Research (AcSIR), New Delhi 110012, India

[5] Department of Marine Geosciences, University of Haifa, 3498838 Haifa, Israel

Published online: 01 March 2019

vertical entrainment, upwelling, Ekman pumping, river discharge, resuspension, and groundwater discharge (*Gao* et al. 2013; *Tan* et al. 2011; *Vahtera* et al. 2005). The growth of phytoplankton is also noticed during heavy dust events due to the readily available Fe content in dust (*Wang* et al. 2012). Based on the observations during 1994–1998, *Fan* et al. (2006) have estimated ~21 Tg/year of Fe deposition in the global oceans due to dust storms. Vincent et al. (2016) have shown that dry dust deposition contributes to almost 10–46% of major dust deposition events over the Mediterranean Sea based on specific sites observations. The global Fe-cycle in terms of Dust-Ocean biogeochemistry-climate interactions is well reviewed in *Jickells* et al. (2005).

The biogeochemistry of the Arabian Sea (AS), which controls the biological production over the region has strong spatial and seasonal variation (McCreary et al. 2009). It changes from eutrophic conditions during monsoon seasons to oligotrophic conditions during inter-monsoon periods (*McCreary* et al. 2009). The semi-annual monsoonal reversal makes it one of the highly productive regions (*Madhupratap* et al. 1996; *Tang* et al. 2002; *Barber* et al. 2001; *Gao* et al. 2013), particularly along the Arabian Peninsula during summer season (*Wiggert* et al., 2005; *Lévy* et al., 2007) and northern part of the AS during winter monsoon season (PrasannaKumar et al. 2010*; Naqvi* et al. 2010). The biological productivity in the AS is related to summer (July–September) and winter (January/February/March) monsoonal flow. During summer, high wind intensity triggers the natural phenomenon (*Barber* et al. 2001) such as Ekman pumping, lateral advection, eddies, and coastal upwelling, which play a prominent role in supplying nutrients to euphotic zone (*Banse* et al. 1996; *Jayakumar* et al. 2001; *Naqvi* et al. 2010). On the other hand, vertical convective mixing due to significant sea surface cooling drives the bloom dynamics during the winter season (*Lee* et al. 2000; *Prakash and Ramesh* 2007). Moreover, on an inter-annual scale, phytoplankton concentration variations during winter are strongly correlated to mixed layer depth fluctuations and mainly controlled by the net heat flux at the air-sea interface (Keerthi et al. 2017). There is lower phytoplankton productivity in March as compared to February, which is associated with the limited vertical mixing in the oceanic layer during March (i.e. away from the realm of active winter convection) due to increased solar radiation-induced layer stratification (*Madhupratap* et al. 1996). February month is generally characterised with high phytoplankton concentration due to natural ocean dynamics (active winter convection as mentioned above) and it is hard to decouple dust effect with ocean dynamics. Therefore, we have focused on the month of March to see the probable association between dust storm and enhanced chlorophyll-a (Chl_a) concentration.

Several studies have been carried out on major dust loading events from African and Asian low-latitude deserts (*Prospero* et al. 1987; *Arimoto* et al. 1990; *Laurent* et al. 2008; *Uno* et al. 2005) and deposition of dust in the northern and western AS (*Li and Ramanathan* 2002; *Zhu* et al. 2007). However, there is a lack of consensus about the impact of dust deposition on the ocean bloom dynamics around the world. For example, *Volpe* et al. *(*2009*)* have suggested the insignificant role of dust to bloom activities over the Mediterranean Sea. On the other hand, a significant positive correlation has been reported between Chl_a and dust deposition over the South yellow Sea and East China Sea (*Tan* et al. 2011). The enhanced AOD during dust storm has also been correlated with increased Chl_a concentration with the lag of 1–4 days in the AS (*Singh* et al. 2008). Recently, *Banerjee and Kumar* (2014) have studied the relationship between atmospheric dust and Chl_a concentrations during winter monsoon over the AS using satellite data and modelling. They showed that the inter-annual variability of phytoplankton concentration during the late winter convection is mainly driven by episodic dust storms. *Kumar* et al. (2010) have also reported annual enhancements of phytoplankton concentration associated with dust-derived nutrient supply over the AS during 1997–2007. They have reported the convection driven nutrient supply coupled with increased dust delivery enhances the phytoplankton concentration during the winter season.

Dust storms usually occurred from April to June over the AS (*Middleton* 1986; *Pease* et al. 1998; *Le'on and Legrand* 2003; *Gautam* et al. 2009). However, there are several dust storm events that also occurred during the early months (January–March) in different years (*Prakash* et al. 2015). One of the prominent dust storms during March 2012 (i.e. 19–21, March) is characterised as a 'super dust storm' as its effects reached as far as Southeast Asia and foothills of Himalayas (*Singh and Beegum* 2013; *Srivastava* et al. 2014; *Alam* et al. 2014). In the present study, we analysed long-term (2003–2016) satellite and reanalysis datasets during March to address the relationship between the bloom dynamics and dust outbreaks over the AS region (15° N–25.5° N and 59° E–70° E). Particularly, we are focused on a dust storm during March 2012 and its association with increased phytoplankton concentration over the AS. The mechanisms associated with the impact of dust activities on primary productivity over AS are also discussed in detail.

Data set and methodology

Moderate resolution imaging spectroradiometer onboard Aqua

Chlorophyll a

Moderate resolution imaging spectroradiometer (MODIS) onboard NASA Aqua and Terra satellites is widely used to

retrieve several data products related to the Earth, Ocean and atmosphere. MODIS is onboard a polar orbiting satellite, passes the equator approximately at 10:30 am/pm local standard time (LST) for Terra and 01:30 am/pm LST for Aqua. In the present study, MODIS-Aqua satellite-derived data is used to study the oceanic parameters such as Chl_a and euphotic depth. The daily oceanic parameters over the AS are obtained from NASA ocean colour web (http://oceancolor.gsfc.nasa.gov/) with the resolution of 4 km for 2003–2016. The empirical-derived algorithm (OC3M) has been used to estimate the Chl_a concentration (Chl_{MA}, mg m^{-3}) using different band ratio of remote sensing reflectance (O'Reilly et al. 2000; Johnson et al. 2013), which is given as follows:

$$Chl_{MA} = 10^{\left(0.2424-2.7423R_{MA}+1.8017R_{MA}^{2}+0.0015R_{MA}^{3}-1.2280R_{MA}^{4}\right)} \quad (1)$$

where $R_{MA} = \log_{10}(R_{rs(443/547)} > R_{rs(490/547)})$ and R_{rs} represents observed reflectance at particular wavelength from Aqua MODIS sensor.

Euphotic depth

Euphotic depth represents the zone where phytoplankton photosynthesis takes place and is known as an important zone in context of ecosystem dynamics (Shang et al. 2011; *Platt and Sathyendranath* 1988). Euphotic depth is estimated from Chl_a (*Morel* et al. 2007) as follows:

$$\text{Euphotic depth} = 34^{*}\ (\text{Chl\_a})^{-0.39} \quad (2)$$

The above approach estimated the euphotic depth within ~ 33% of in situ observations (*Lee* et al. 2007). Details of algorithm, associated uncertainties and validation can be found elsewhere (Lee et al. 2005; Morel et al. 2007; *Lee* et al. 2010). We have used daily euphotic depth data over the AS for March 2012 on a 4-km spatial resolution.

Aerosol optical depth

MODIS onboard Aqua satellite is also used to obtain the level 3 daily aerosol data product (MYD08_D3_6_Aerosol_Optical_Depth_Land_Ocean_Mean) from giovanni.gsfc.nasa.gov/ platform with the $1^0 \times 1^0$ resolution. In the present work, AOD_{550} from collection 6 is used over the AS for the period of 2003 to 2016. The uncertainty associated with MODIS-AOD over land and ocean are ± (0.05 + 0.15*AOD) and ± (0.03 + 0.05*AOD), respectively (*Levy* et al. 2010; *Remer* et al. 2002).

Sea surface temperature

A new generation global sea surface temperature (SST) is provided by the group of high resolution of sea surface temperature with different levels such as level 2P, level 3, and level 4. The level 4 data (derived from L2P products) is generated from multiple satellite data sets using optimal interpolation, which provides gridded and gap-free products. The daily data is obtained from the web platform of GHRSST (http://www.ghrsst.org) with the resolution of $0.011^0 \times 0.011^0$ for March 2003–2016.

Modern-Era Retrospective analysis for Research and Applications-2

Modern-Era Retrospective analysis for Research and Applications (MERRA-2) is a satellite constrained reanalysis model developed by the Global Modelling and Assimilation Office (GMAO) of NASA (*Rienecker* et al. 2011). GOCART module is being used to simulate the different aerosols (dust, black carbon, sulfate, sea salt and organic carbon) using GEOS-5 model in the MERRA-2 reanalysis system (*Buchard* et al. 2016). In the MERRA-2 simulations, aerosols are treated as externally mixed particles and are represented by five different layers to predict the mass-mixing ratio of particles in the five size bins, i.e. 0.1–1, 1–1.8, 1.8–3, 3–6 and 6–10 μm radius of particle (*Bosilovich* et al. 2016). In the present study, total dust-dry deposition flux is calculated by the sum of the deposition fluxes in the individual dust bins at spatial resolution of $0.5^0 \times 0.625^0$. The total dust-dry deposition flux is then used to estimate the deposition of Fe in the AS. Fe deposition is estimated as 3.5% of total dry deposition (*Mahowald* et al. 2005; *Gao* et al. 2003) and that the bioavailable component only accounts for 0.4% of it (*Srinivas* et al. 2011).

MERRA-2 derived hourly simulated clear sky radiation data (e.g. shortwave radiative flux at surface) with and without aerosols are used to estimate clear sky shortwave aerosols direct radiative forcing at ocean surface (SRF) (Bali et al. 2017) during March 2003–2016. The wind vector at 850 and 1000 hPa and wind stress data are also obtained from MERRA-2 during March 2012. We estimated the Ekman mass transport following *Smitha* et al. (2014) by dividing the meridional wind stress by coriolis parameter. Meridional wind stress is estimated by the multiplication of meridional wind air density and drag coefficient. Coriolis parameter is obtained as $2\,\Omega \sin \Phi$, where Ω denotes the angular frequency (radian/s) of the Earth and Φ represents the latitude.

ERA-interim

ERA-interim is a part of global atmospheric reanalysis data product provided by European Centre for Medium-Range Weather Forecasts (ECMWF). Twelve hourly 4D-Var data assimilation methodology and T255 spectral model with the 60 vertical model levels are the core component of ERA-interim (Lawrence et al. 2015). This dataset provides the four

analyses per day on 00, 06, 12 and 18 UTC. Daily vertical profiles of wind components (u and v) and specific humidity data (1000–850 hPa) along with turbulent heat fluxes (latent heat flux and sensible heat flux) at surface are obtained for March 2012 at $0.125^{\circ} \times 0.125^{\circ}$ horizontal resolution. Detail information about ERA-interim data and its availability can be found in Dee et al. (2011) and at ECMWF website (http://apps.ecmwf.int/).

Correlation analysis

We have used 30 days data to calculate temporal Pearson's correlation coefficients between spatially averaged (over the AS) daily estimated dust deposition anomaly and Chl_a concentration anomaly as a function of forward lag (in days) during March 2012. The daily anomalies were calculated with respect to March 2012 mean. The spatial map of Pearson's correlation coefficients is also derived using collocated daily estimated dust deposition anomaly and Chl_a concentration anomaly over the AS. The spatial correlation map is not created using 30 days data for all pixels because of unavailability of continuous 30 days data from MODIS over several pixels.

Results

A dust storm is observed over the Middle East and southwest Asia during March 2012 by Earth observatory NASA (Figs. 1 a and b). These figures show a plume of dust that stretches across the AS from the coast of Oman to India. To quantify the relative strength of the March 2012 dust storm with respect to others years, we analysed the estimated dust deposition rate over the AS during 2003–2016. Figure 1 c shows the yearly variation of estimated dry dust deposition rate for March month from 2003 to 2016 averaged over the AS (15° N–25.5° N and 59° E–70° E). Figure 1 c clearly shows a maximum dust deposition rate in March 2012 (~ 13 mg m^{-2} day^{-1}). Similarly, Fig. 1 d shows spatial distribution of dust deposition anomaly over the AS for March 2012. We have analysed anomalies of observed (2012) vs. 14 years mean data for the month of March in this study. A substantial positive anomaly of dust deposition rate ($\sim$6–12 mg m^{-2} day^{-1}) during March 2012 is observed, which is also established from the monthly variation (Jan–Apr) of dry dust deposition rate from 2003 to 2016 over the AS (Fig. S1, supplementary material).

Figures 2 a and b show the spatial distribution of mean Chl_a concentration over the AS for March during 2003–2016 and 2012 anomaly, respectively. In general, the northern part of AS shows high mean Chl_a concentration (Fig. 2 a), but positive Chl_a anomalies (Fig. 2 b) are observed over the central AS (18°–22° N and 60°–68° E) during March 2012. Substantial large positive anomalies of Chl_a ($\sim$4–12 mg m^{-3}) accompanied with positive estimated dust deposition rate anomalies ($\sim$6–12 mg m^{-2} day^{-1}) are observed over the central AS (Fig. 2 b and Fig. 1 d). A negative Chl_a anomaly can also be seen in the north of the basin relatively closer to the coastal region and in the north of the positive anomaly region. Due to sufficient availability of nutrient and coastal upwelling (Naqvi et al. 2010), blooms near the coastal region are common. However, the enhancement of Chl_a concentration in central region during March 2012 warrants comprehensive analysis.

Figure 3 shows that the AOD and the estimated dust deposition both have similar trends and reach their maximum ($\sim$0.8 and $\sim$52 mg m^{-2} day^{-1}, respectively) on the 20th of March 2012 (Figs. 3 b and c). However, the highest peak of Chl_a ($\sim$9.4 mg m^{-3}) is observed on the 24th of March 2012, after a lag of 4 days from the dust storm event. Similar increased chlorophyll concentration after a lag of 1 to 4 days of dust storm has also been reported earlier over the AS (*Singh* et al. 2008; *Banerjee and Kumar* 2014). In order to know the exact lag (days) between dust deposition and Chl_a concentration, we have further used a lag correlation analysis to see when we get the maximum correlation. Figure 4 a shows Pearson's correlation coefficients between spatially averaged daily dust deposition anomaly and Chl_a concentration anomaly over the AS as a function of forward lag (in days) during March 2012. The maximum correlation ($\sim$0.58 significant at 95% CI) between Chl_a and estimated dust deposition rate are found at 4 days lag. Further, Fig. 4 b shows the spatial distribution of correlation coefficients between Chl_a and dust deposition rate (daily anomalies) at 4 days forward lag during March 2012. It again shows high correlation coefficients (> 0.6) over the positive Chl_a anomalies region over the AS.

Figure 5 shows the time series of the daily mean (2003–2016) and 2012 anomaly in (a) SST and (b) shortwave surface radiative forcing (SRF) during March averaged over the AS. Results show a continuous increase in mean SST as the month progressed, which is related to the annual cycle of solar radiation. Moreover, Fig. 5 a shows that the March 2012 is in general associated with lower SST as compared to 14 years mean. A sharp reduction in SST ($\sim$0.8 °C) is visible in a span of 4 days during the 17th–21st of March 2012. The dip in SST-anomaly is also consistent with a dip in SRF occurring on the 20th of March. Moreover, the surface latent heat flux (negative values indicate ocean to atmosphere heat transfer) also shows maximum value on the 20th of March (Fig. 6 a), which is also consistent with the dip in SST. A somewhat similar, reduction in SST is also observed on the 12th of March which may be associated with another relatively weak dust outbreak with a nearly similar pattern of latent heat flux with mild peak. However, the effect is not so prominent and may be because of a different history where SST may be decreasing since third to 12th of March.

The ocean surface latent heat flux is directly proportional to the product of wind speed at a 10-m level (above water

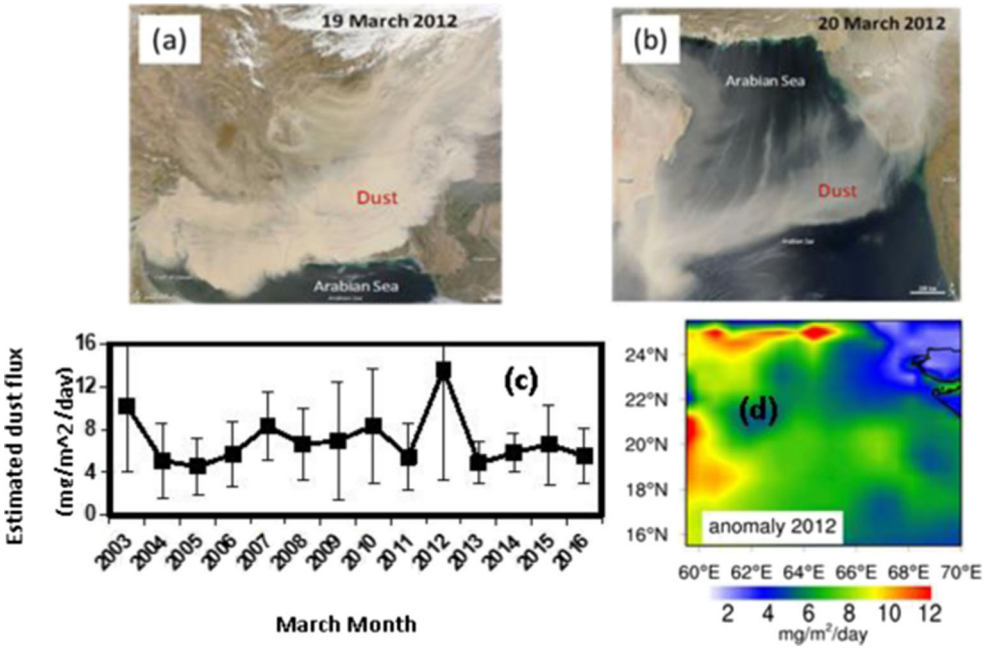

Fig. 1 MODIS (Aqua) images showing **a** heavy dust plume covering the Gulf, Iraq, Iran, Pakistan and India on the 19th of March 2012 and **b** dust plume reaching over Arabian Sea on the 20th of March 2012. **c** Yearly (March month only) variation of estimated dry dust deposition averaged over the Arabian Sea (15° N–25.5° N and 59° E–70° E) during 14 consecutive years (2003–2016) and **d** spatial distribution of estimated dust deposition anomaly for March 2012 with respect to 14 years (2003–2016) mean of March month

surface) and specific humidity difference between ocean surface and at some specific height above the water surface (Bradley et al. 1991; Zhang and McPhaden 1995). We have taken 1000 and 850 hPa as two reference levels for calculation of humidity difference in this study. Figure 6 b shows that this product also has a maximum on the 20th of March. In general, the high surface wind speed over ocean increases the turbulent heat flux, which is manifested in Fig. 6 a. Therefore, the reduced SST could be understood as the combination of the radiative effect of dust loaded atmosphere on incoming shortwave solar radiation and sudden increase in latent heat flux due to increased surface wind speed during dust outbreak event. The role of direct radiative effect of dust and associated latent heat fluxes changes on SST variability has been shown

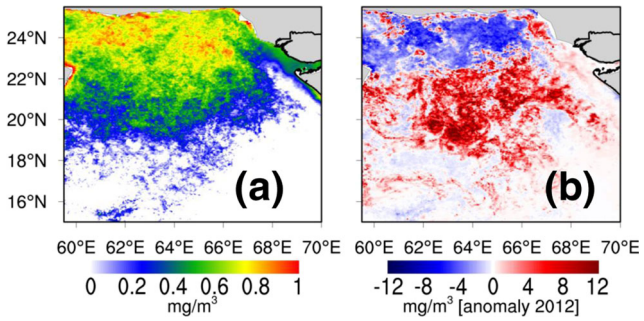

Fig. 2 **a** Left panel shows the mean (2003–2016) spatial variability of satellite derived Chl_a (mg m^{-3}, plotted as logarithmic of actual values, in colour bar) of March month over the Arabian Sea and **b** right panel represents the spatial distribution of Chl_a anomaly for the March 2012 as compared to 14 years (2003–2016) March mean. The anomaly is the difference of Chl_a concentration of March, 2012 and that of climatological mean for 2003–2016 (for March month only)

in various studies over tropical Atlantic Ocean (Lau and Kim 2007; Foltz and McPhaden 2008; Evan et al. 2011). The mean ocean mixed layer depth is < 30 m over the AS during the month of March (Fig. 5 in de Boyer Montégut et al. 2004). Therefore, over such a shallow mixed layer depth region, SST decrease may facilitate nutrient upwelling by driving convection processes (due to density differences between surface and subsurface ocean water) that lead to the injection of nutrients up into the surface waters (*Madhupratap* et al. 1996; *Hofmann* et al. 2011; *Poll* et al. 2013), which may favour growth of phytoplankton. Euphotic depth anomaly time series is also consistent with the SST result (supplementary Fig. S3).

Chl_a enhancement is linked to several other factors such as coastal upwelling, wind stress, and Ekman mass transport. To quantify the impact of Ekman mass transport on phytoplankton concentration in the central AS, we analysed spatial and temporal variation of Ekman mass transport (kg/m/s) anomaly and dry dust deposition rate (mg m^{-2} day^{-1}) anomaly (Fig. 7) during the dust event (19th–21st of March). Ekman mass transport < − 2000 kg/m/s is considered as a strong Ekman mass transport, which results in strong upwelling and nutrient transport to the Sea (*Smitha* et al. 2014). The strong Ekman mass transport (< − 2000 kg/m/s) during dust storm (20th of March 2012) has been observed from northern coastal AS region to the central AS. Moreover, the northern coastal region of the AS also received maximum dust deposition ~ 90–100 (mg m^{-2} day^{-1}). Therefore, Ekman mass transport may also be responsible for the transport of dust-abundant and nutrient rich coastal water to the central AS region. This process is possibly responsible for a deficient Chl_a and a negative anomaly in the northern region of the basin (Fig. 2 b).

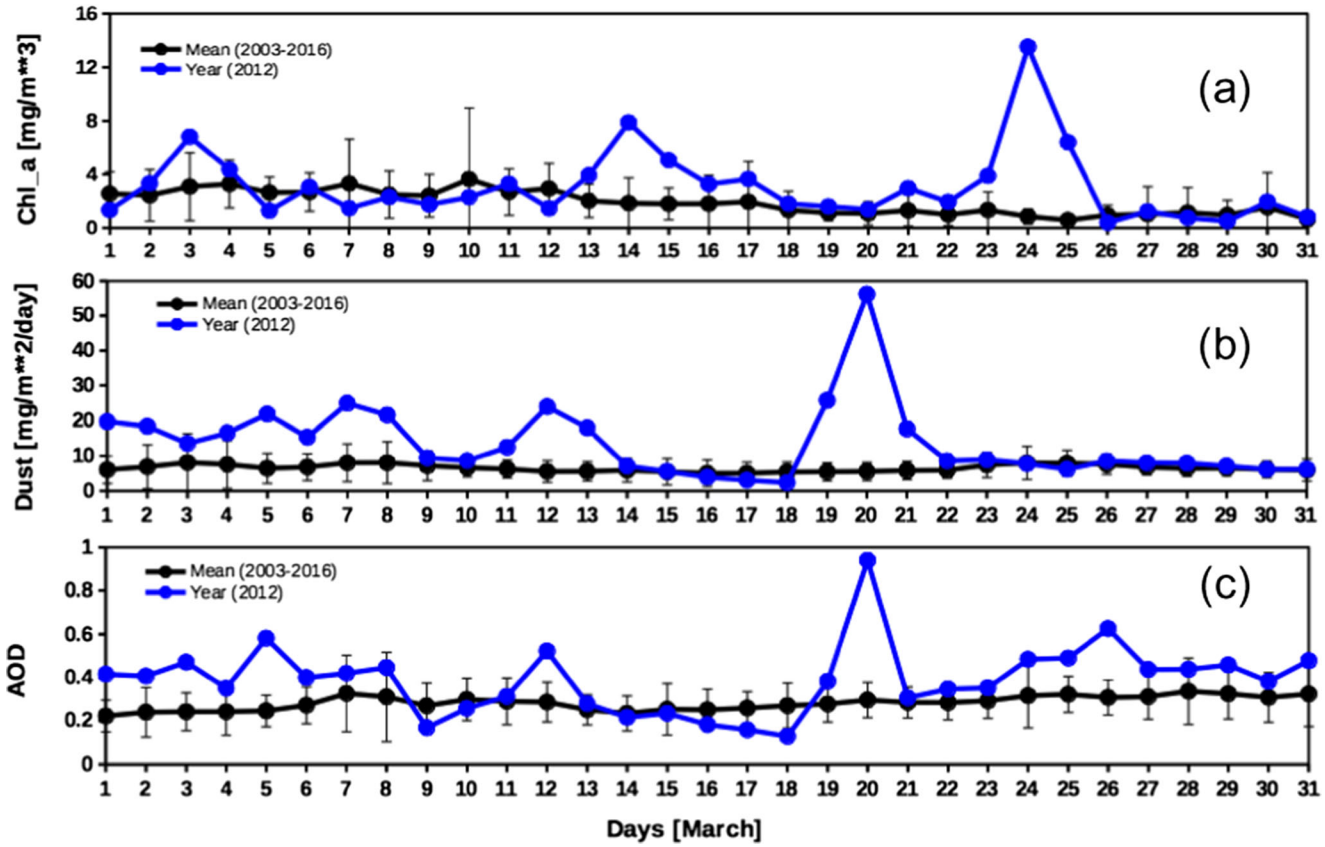

Fig. 3 Daily time series of year 2012 and 14 years (2003–2016) mean of **a** Chl_a (mg m^{-3}), **b** estimated dust deposition rate (mg m^{-2} day^{-1}) and **c** AOD during March month averaged over the Arabian Sea (150° N–25.50° N and 590° E–700° E). Black and blue colours represent mean and individual values, respectively

Discussions and summary

The AS is considered as an important sink region for the dust originated from the Middle East and southwest Asia during the dust storm events. The dust aerosols originating from these regions have high Fe content which reaches > 2 μg/m^3 during dusty conditions (*Najafi* et al. 2014; *Alghamdi* et al. 2015). Wang et al. (2012) shows large Fe concentration (> 0.5 μg/m^3) over the AS due to the outflow of dust from Arabian, Lut and Thar deserts. The AS (especially western and northern part)

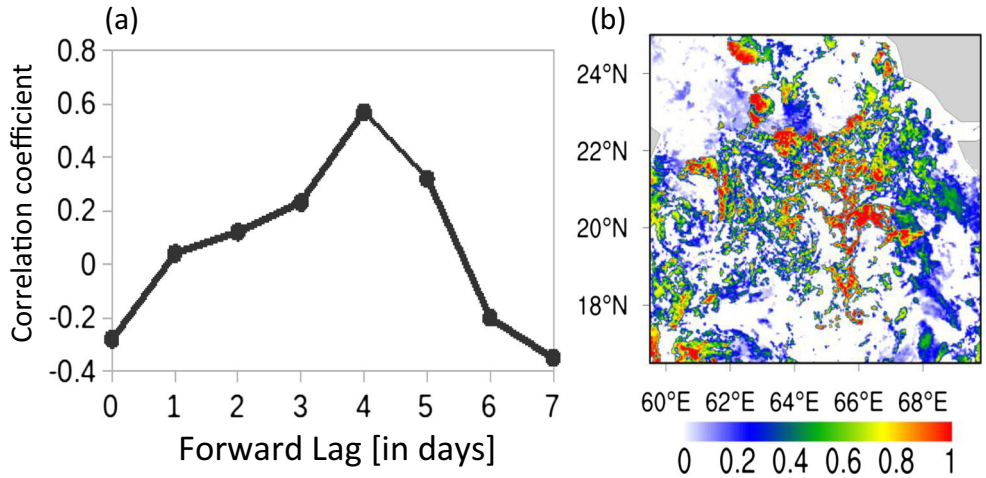

Fig. 4 **a** Pearson's correlation coefficients between averaged Chl_a and averaged estimated dust deposition rates daily anomalies over the Arabian Sea (15° N–25.5° N and 59° E–70° E) as a function of forward lag (days) during March 2012. The correlation coefficient at 4 days lag is significant at 95% confidence interval (CI), whereas others are insignificant (i.e. $p > 0.05$). **b** Spatial distribution of correlation coefficient between Chl_a and dust deposition rates daily anomalies at 4 days forward lag during March 2012. Fig. S2 shows region where correlations are significant at 95% CI. The daily anomalies were calculated with respect to March 2012 mean

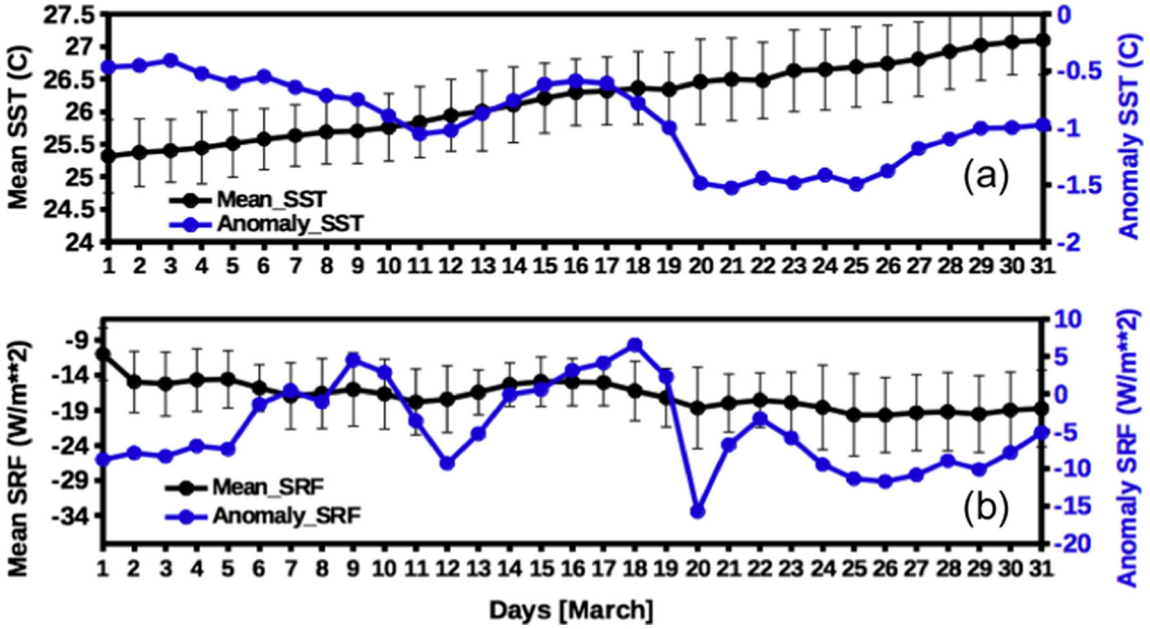

Fig. 5 Daily time series of anomaly and 14 years (2003–2016) mean of **a** sea surface temperature (SST, °C) and **b** shortwave surface radiative forcing (SRF, W/m^2) during March month averaged over the AS (15° N–25.5° N and 59° E–70° E). Blue and black colours represent the anomaly and mean values, respectively

experiences maximum atmospheric dust deposition (*Prospero* et al. 2002; *Zhu* et al. 2007) and is found to be one of the most productive regions of the ocean (*Barber* et al. 2001). High nutrients content has also been reported in this region (*Singh* et al. 2008; *Naqvi* et al. 2010). Dust is also a potential source of other essential nutrients such as nitrogen and phosphorous (Prakash et al. 2016; Ramaswamy et al. 2017) which are important for marine life. The compounds of Fe, nitrogen and phosphorus were identified in dust samples from the Arabian Peninsula (Prakash et al. 2016). Mainly, the mixing of dust with anthropogenic pollution during transport process brings N and P content in the dust. Ramaswamy et al. (2017) have shown a significant amount of ions of N and P in rainwater samples along the west coast of India. Therefore, the dust storm plays an important role in providing the essential nutrients to the AS.

The significant association between the phytoplankton bloom and the aerosol optical depth has been established in the AS (*Banerjee and Kumar* 2014) like several other regions of the ocean (*Gabric* et al. 2002; *Calil* et al. 2011; *Han* et al. 2011; *Gallisai* et al. 2014). It may be argued that the atmospheric dust deposition can be the prime source of dissolved Fe in the open ocean, but in the continental margins, it is the sedimentary sources that dominate (*Moore and Braucher* 2008). However, the Fe rich dust aerosols from the west and southwest Asia can certainly provide essential micronutrients in the dissolved ocean water of the AS to boost the phytoplankton productivity in the region (*Singh* et al. 2008). Several studies have shown the role of dissolution of Fe in ocean waters due to the dust transportation (Hand et al. 2004; *Buck* et al. 2006; *Journet* et al. 2008; *Baker and Croot* 2010; *Takahashi* et al. 2011; *Han* et al.

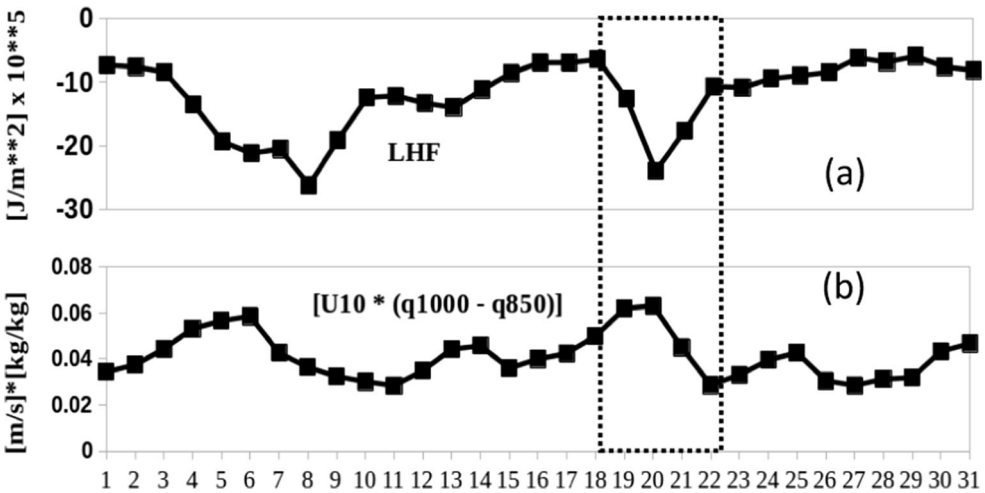

Fig. 6 Daily time series of latent heat flux (LHF) (upper panel) and product of wind speed at 10 m above ocean surface (U_{10}) and specific humidity difference at 1000 and 850 hPa ($q_{1000} - q_{850}$) during March month averaged over the AS (15° N–25.5° N and 59° E–70° E)

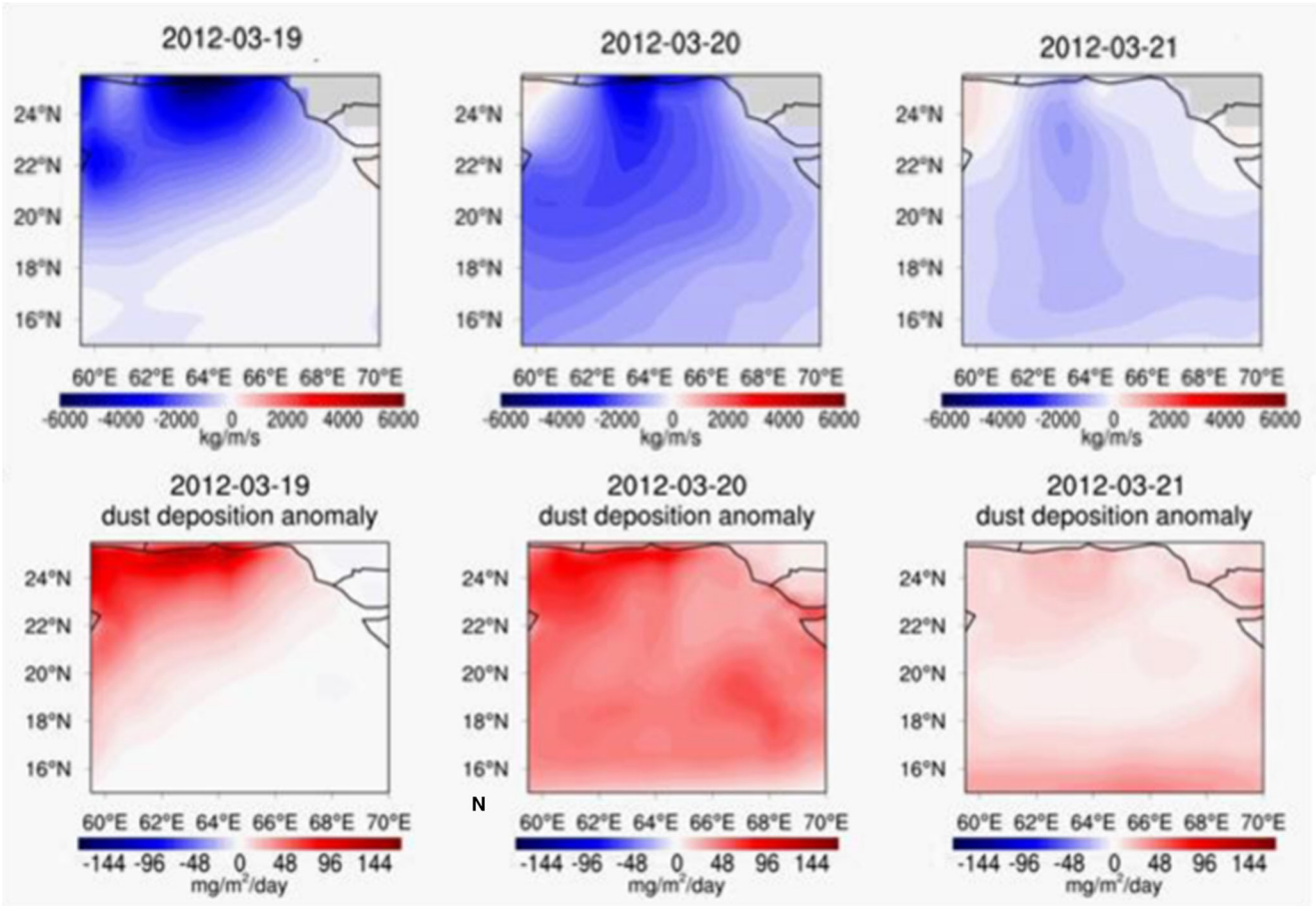

Fig. 7 Spatial and temporal variation Ekman mass transport (kg/m/s) anomaly and dry dust deposition rate (mg m^{-2} day^{-1}) anomaly during super dust event (19th–21st of March 2012). Both, Ekman mass transport and dust deposition rate are prominent on all 3 days with maximum on the 20th of March. Anomaly is calculated as daily values minus March 2012 mean

2011; *Conway and John* 2014). However, a recent study by *Banerjee and Kumar* (2014) has found only 8 (out of 45) dust storms followed by enhanced phytoplankton concentration over the AS during winter monsoon of 2002–2011. This finding imposes an interesting question about the non-association of other dust storms with phytoplankton bloom over the AS, which need to be addressed.

The daily average dry dust deposition rate plotted for the entire month of March 2012 in Fig. 3 shows that the daily estimated dust deposition increased drastically from ~ 2.5 mg m^{-2} day^{-1} on 18th of March to ~ 52 mg m^{-2} day^{-1} on the 20th of March due to the dust storm which settled down to normal level only on 22nd of March (~ 8.6 mg m^{-2} day^{-1}). A similar scenario is also observed during the 10th–14th of March, when daily estimated dust deposition varying between ~ 7–22 mg m^{-2} day^{-1} with peak concentration on 12th of March. Such a rapid increase in dust deposition was also observed by Han et al. (2011) during the Asian dust storm of April 2001 in the North Pacific Ocean. The estimated Fe deposition rate ("Modern-Era Retrospective analysis for Research and Applications-2") is found 1.85 mg m^{-2} day^{-1} on the 20th of March. It amounts to about 4.41 μg m^{-2} day^{-1} of soluble aeolian Fe in the surface layer of the AS which is equivalent to about 133 nM of Fe. Such a high Fe concentration with other available nutrients such as N and P (not quantified in this paper) in the AS could trigger the rapid increase in chlorophyll concentration. *Wells* (2003) has shown that even 2 nM increase in Fe concentration can stimulate phytoplankton blooms. This can be noticed from our results which show that the Chl_a concentration increased more than four times from the 20th to 24th of March 2012.

In addition to bio-available nutrient supply, the dust storm of March 2012 is also associated with a decrease of about 0.8 °C in the SST over the AS. A similar type of decrease in SST of ~ 0.3 °C is also associated with the 12th of March dust storm. The decrease in SST could destabilise stratified layers in the ocean and may enhance the vertical mixing which could supply micronutrients from the deeper ocean to euphotic zone (*Hofmann* et al. 2011). *Poll* et al. (2013) shows an inverse relationship between SST and primary productivity over the Atlantic Ocean and found that a 0.5 °C change in SST would cause the 11% change in daily primary productivity in upper 50 m.

From all the results and discussion presented above, we can summarise that the dust storm of March 2012 was associated with different driving mechanisms for enhanced phytoplankton concentration in the central AS. This particular dust storm provides favourable conditions for phytoplankton bloom, i.e. micronutrient availability by dust deposition and nutrient upwelling by SST cooling. These mechanisms are associated with dust outbreaks that modulate the ocean productivity through chemical and physical changes. It is possible that every dust storm occurring in this region could not bring all the above-mentioned changes that are responsible for chlorophyll enhancement during weak winter convection conditions. This could explain why not all the dust storms are followed with phytoplankton bloom over the AS (Banerjee and Kumar 2014). The episodic nature of atmospheric deposition (which may provide essential nutrients) needs to be considered in ocean biogeochemistry models for better understanding of ocean productivity processes (Guieu et al. 2014). In summary, we have shown an association between a dust storm and an event of anomalous biological production in the AS. We suggest that the enhanced biological production results from the superposition of two main complementary processes, i.e. deposition of atmospheric nutrients at the surface water and enhancement of nutrient availability at the surface water due to dust-induced SST cooling that reduces water column stratification. However, long term in situ and satellite observations coupled with better ocean models are required to establish the comprehensive relationship between dust deposition and Chl_a concentration over AS region.

Acknowledgments We acknowledge the National Aeronautics and Space Administration (NASA) and Giovanni (giovanni.sci.gsfc.nasa.gov) for MODIS and MERRA-2 datasets used in this research. A part of this work was sponsored by ISRO-GBP (Indian Space Research Organisation—Geosphere Biosphere Programme) under ARFI (Aerosol Radiative Forcing over India) project. We are thankful to Director, NPL for his encouragement and support. We are grateful to the two anonymous referees for their valuable suggestions in improving this paper.

Funding information This study was financially supported by the Department of Science and Technology, Government of India as an INSPIRE Faculty (DST/INSPIRE/04/2015/003253).

References

Alam K, Trautmann T, Blaschke T, Subhan F (2014) Changes in aerosol optical properties due to dust storms in the Middle East and Southwest Asia. Remote Sens Environ 143:216–227

Albrecht BA (1989) Aerosols, cloud microphysics, and fractional cloudiness. Science 245:1227–1230

Alghamdi MA, Almazroui M, Shamy M, Redal MA, Alkhalaf AK, Hussein MA, Khoder MI (2015) Characterization and elemental composition of atmospheric aerosol loads during springtime dust storm in western Saudi Arabia. Aerosol Air Qual Res 15:440–453

Arimoto, R., R. A. Duce, and B.J. Ray (1990), Concentrations, sources and air-sea exchange of trace elements in the atmosphere over the Pacific Ocean, in Riley et al. (eds.). Chem Oceanogr, 10, 107–149

Banse K, Sumitra V, Madhupratap M (1996) On the possible causes of the seasonal phytoplankton blooms along the west coast of India. Ind J Marine Sci 25:283–289

Banerjee P, Kumar SP (2014) Dust-induced episodic phytoplankton blooms in the Arabian Sea during winter monsoon. J Geophys Res Oceans 119:7123–7138. https://doi.org/10.1002/2014JC010304

Baker AR, Croot PL (2010) Atmospheric and marine controls on aerosol iron solubility in seawater. Mar Chem 120:4–13. https://doi.org/10.1016/j.marchem.2008.09.003

Bali K, Mishra AK, Singh S (2017) Impact of anomalous forest fire on aerosol radiative forcing and snow cover over Himalayan region. Atmos Environ 150:264–275

Barber RT, Marra J, Bidigare RC, Codispoti LA, Halpern D, Johnson Z, Latasa M, Goericke R, Smith SL (2001) Primary productivity and its regulation in the Arabian Sea during 1995. Deep-Sea Res II Top Stud Oceanogr 48:1127–1172

Bosilovich, M. G., R. Lucchesi, and M. Suarez (2016), MERRA-2: File Specification GMAO Office Note No 9 (Version 1.1), 73 pp, available from http://gmao.gsfc.nasa.gov/pubs/officenotes. Accessed 21 March 2016

Bradley EF, Coppin PA, Godfrey JS (1991) Measurements of sensible and latent heat flux in the western equatorial Pacific Ocean. J Geophys Res Oceans 96(S01):3375–3389

Buchard V, da Silva AM, Randles CA, Colarco P, Ferrare R, Hair J, Hostetler C, Tackett J, Winker D (2016) Evaluation of the surface PM2.5 in version 1 of the NASA MERRA aerosol reanalysis over the United States. Atmos Environ 125:100–111

Buck CS, Landing WM, Resing JA, Lebon GT (2006) Aerosol iron and aluminum solubility in the northwest Pacific Ocean: results from the 2002 IOC cruise. Geochem Geophys Geosyst 7:Q04M07. https://doi.org/10.1029/2005GC000977

Calil PHR, Doney SC, Yumimoto K, Eguchi K, Takemura T (2011) Episodic upwelling and dust deposition as bloom triggers in low-nutrient, low-chlorophyll regions. J Geophys Res 116:C06030. https://doi.org/10.1029/2010JC006704

Conway TM, John SG (2014) Quantification of dissolved iron sources to the North Atlantic Ocean. Nature 511:212–215. https://doi.org/10.1038/nature13482

de Boyer Montégut C, Madec G, Fischer AS, Lazar A, Iudicone D (2004) Mixed layer depth over the global ocean: An examination of profile data and a profile based climatology. J Geophys Res Oceans 109(C12):C12003

Dee DP, Uppala SM, Simmons AJ, Berrisford P, Poli P, Kobayashi S, Andrae U, Balmaseda MA, Balsamo G, Bauer P, Bechtold P, Beljaars ACM, van de Berg L, Bidlot J, Bormann N, Delsol C, Dragani R, Fuentes M, Geer AJ, Haimberger L, Healy SB, Hersbach H, Hólm EV, Isaksen L, Kållberg P, Köhler M, Matricardi M, McNally AP, Monge-Sanz BM, Morcrette JJ, Park BK, Peubey C, de Rosnay P, Tavolato C, Thépaut JN, Vitart F (2011) The ERA-interim reanalysis: configuration and performance of the data assimilation system. Q J Roy Meteor Soc 137:553–597

Duce RA, Tindale NW (1991) Atmospheric transport of iron and its deposition in the ocean. Limnology Oceano 36(8):1715–1726

Evan AT, Foltz GR, Zhang D, Vimont DJ (2011) Influence of African dust on ocean-atmosphere variability in the tropical Atlantic. Nat Geosci 4(11):762–765

Fan SM, Moxim WJ, Levy H II (2006) Aeolian input of bio available iron to the ocean. Geophys Res Lett 33:L07602. https://doi.org/10.1029/2005GL024852

Foltz GR, McPhaden MJ (2008) Impact of Saharan dust on tropical North Atlantic SST. J Clim 21(19):5048–5060

Fung IY, Meyn SK, Tegen II, Doney SC, John JG, Bishop JKB (2000) Iron supply and demand in the upper ocean. Glob Biogeochem Cycles 14(2):697–700

Gabric AJ, Cropp R, Ayers GP, McTainsh G, Braddock R (2002) Coupling between cycles of phytoplankton biomass and aerosol optical depth as derived from SeaWiFS time series in the Subantarctic Southern Ocean. Geophys Res Lett 29(7):1112. https://doi.org/10.1029/2001GL013545

Gallisai R, Peters F, Volpe G, Basart S, Baldasano JM (2014) Saharan dust deposition may affect phytoplankton growth in the Mediterranean Sea at ecological time scales. PLoS One *9*(10):e110762

Gao Y, Xu G, Zhan J, Zhang J, Li W, Lin Q, Chen L, Lin H (2013) Spatial and particle size distributions of atmospheric dissolvable iron in aerosols and its input to the Southern Ocean and coastal East Antarctica. J Geophys Res Atmos *118*(12):634–12, 648. https://doi.org/10.1002/2013JD020367

Gao Y, Fan S-M, Sarmiento JL (2003) Aeolian iron input to the ocean through precipitation scavenging: a modeling perspective and its implication for natural iron fertilization in the ocean. J Geophys Res 108(D7):4221. https://doi.org/10.1029/2002JD002420

Gautam R, Liu Z, Singh RP, Hsu NC (2009) Two contrasting dust-dominant periods over India observed from MODIS and CALIPSO data. *Geophys Res Lett* 36:L06813. https://doi.org/10.1029/2008GL036967

Goudie AS, Middleton NJ (2001) Saharan dust storms: nature and consequences. Earth-Sci Rev 56:179–204

Guieu, C., Aumont, O., Paytan, A., Bopp, L., Law, C. S., Mahowald, N., ... & Wagener, T. (2014). The significance of the episodic nature of atmospheric deposition to low nutrient low chlorophyll regions. Glob Biogeochem Cycles, 28(11), 1179–1198

Han Y, Zhao T, Song L, Fang X, Yin Y, Deng Z, Wang S, Fan S (2011) A linkage between Asian dust, dissolved iron and marine export production in the deep ocean. Atmos Environ 45:4291–4298

Hand JL, Mahowald NM, Chen Y, Siefert RL, Luo C, Subramaniam A, Fung I (2004) Estimates of atmospheric processed soluble iron from observations and a global mineral aerosol model: biogeochemical implications. J Geophys Res 109:D17205. https://doi.org/10.1029/2004JD004574

Hofmann M, Worm B, Rahmstorf S, Schellnhuber HJ (2011) Declining ocean chlorophyll under unabated anthropogenic CO2 emissions. Environ Res Lett 6(3):034035

Hutchins DA, Bruland KW (1998) Iron-limited diatom growth and Si:N uptake ratios in a coastal upwelling regime. Nature 393:561–564

Jayakumar D, Naqvi SW, Narvekar P, George M (2001) Methane in coastal and offshore waters of the Arabian Sea. Mar Chem 74:1–13. https://doi.org/10.1016/S0304-4203(00)00089-X

Jickells TD, An ZS, Andersen KK, Baker AR, Bergametti G, Brooks N, Cao JJ, Boyd PW, Duce RA, Hunter KA, Kawahata H (2005) Global iron connections between desert dust, ocean biogeochemistry, and climate. Science 308(5718):67–71

Johnson R, Strutton PG, Wright SW, McMinn A, Meiners KM (2013) Three improved satellite chlorophyll algorithms for the Southern Ocean. J Geophy Res Oceans *118*(7):3694–3703

Journet E, Desboeufs KV, Caquineau S, Colin JL (2008) Mineralogy as a critical factor of dust iron solubility. Geophys Res Lett 35:L07805. https://doi.org/10.1029/2007GL031589

Keerthi, M. G., Lengaigne, M., Lévy, M., Vialard, J., Parvathi, V., de Boyer Montégut, C., ... & Muraleedharan, P. M. (2017). Physical control of interannual variations of the winter chlorophyll bloom in the northern Arabian Sea. Biogeosciences, 14(15), 3615, 3632

PrasannaKumar S, Roshin RP, Narvekar J, Kumar PKD, Vivekanandan E (2010) What drives the increased phytoplankton biomass in the Arabian Sea? Curr Sci 99:101–106

Laurent B, Marticorena B, Bergametti G, Leon JF, Mahowald NM (2008) Modeling mineral dust emissions from the Sahara desert using new surface properties and soil database. J Geophys Res 113:D14218. https://doi.org/10.1029/2007JD009484

Lau KM, Kim KM (2007) Cooling of the Atlantic by Saharan dust. Geophys Res Lett 34(23)

Lawrence ZD, Manney GL, Minschwaner K, Santee ML, Lambert A (2015) Comparisons of polar processing diagnostics from 34 years of the ERA-interim and MERRA reanalyses. Atmos Chem Phys 15:3873–3892

Le'on J-F, Legrand M (2003) Mineral dust sources in the surroundings of the north Indian Ocean. Geophys Res Lett 30(6):1309. https://doi.org/10.1029/2002GL016690

Lee CM, Jones BH, Brink KH, Fischer AS (2000) The upper-ocean response to monsoonal forcing in the Arabian Sea: seasonal and spatial variability. Deep-Sea Res II Top Stud Oceanogr 47:1177–1226

Lee Z, Du K, Arnone R, Liew A, Penta B (2005) Penetration of solar radiation in the upper ocean: a numerical model for oceanic and coastal waters. J Geophys Res 110:C09019

Lee Z, Weidemann A, Kindle J, Arnone R, Carder KL, Davis C (2007) Euphotic zone depth: its derivation and implication to ocean-color remote sensing. J Geophys Res 112:C03009

Lee Z, Arnone R, Hu C, Werdell PJ, Lubac B (2010) Uncertainties of optical parameters and their propagations in an analytical ocean color inversion algorithm. Appl Opt 49:369–381

Lévy M, Shankar D, André JM, Shenoi SSC, Durand F, de Boyer Montégut C (2007) Basin-wide seasonal evolution of the Indian Ocean's phytoplankton blooms. J Geophys Res Oceans 112(C12)

Levy RC, Remer LA, Kleidman RG, Mattoo S, Ichoku C, Kahn R, Eck TF (2010) Global evaluation of the Collection 5 MODIS dark-target aerosol products over land. Atmos Chem Phys 10(21):10399–10420

Li F, Ramanathan V (2002) Winter to summer monsoon variation of aerosol optical depth over the tropical Indian Ocean. J Geophys Res 107:4284. https://doi.org/10.1029/2001JD000949

Lohmann U, Feichter J (2005) Global indirect aerosol effects: a review. Atmos Chem Phys 5:715–737

Madhupratap M, Prasanna KS, Bhattathiri PMA, Dileep KM, Raghukumar S, Nair KKC, Ramaiah N (1996) Mechanism of the biological response to winter cooling in the northeastern Arabian Sea. Nature 384:549–552

Mahowald NM, Baker AR, Bergametti G, Brooks N, Duce RA, Jickells TD, Kubilay N, Prospero JM, Tegen I (2005) Atmospheric global dust cycle and iron inputs to the ocean. Glob Biogeochem Cycles 19:GB4025. https://doi.org/10.1029/2004GB002402

McCreary JP, Murtugudde R, Vialard J, Vinayachandran PN, Wiggert JD, Hood RR, Shankar D, Shetye S (2009) Biophysical processes in the Indian Ocean. Indian Ocean biogeochemical processes and ecological variability. Geophys Monogr Ser 185:9–32

Middleton NJ (1986) A geography of dust storms in Southwest Asia. Int J Climatol 6:183–196

Moore JK, Braucher O (2008) Sedimentary and mineral dust sources of dissolved iron to the world ocean. Biogeosci. 5:631–656

Morel A, Claustre H, Antoine D, Gentili B (2007) Natural variability of bio-optical properties in case 1 waters: attenuation and reflectance within the visible and near-UV spectral domains, as observed in South Pacific and Mediterranean waters. Biogeosciences 4:913–925

Najafi MS, Khoshakhllagh F, Zamanzadeh SM, Shirazi MH, Samadi M, Hajikhani S (2014) Characteristics of TSP loads during the Middle East springtime dust storm (MESDS) in Western Iran. Arab J Geosci 7(12):5367–5381

Naqvi SWA, Moffett JW, Gauns MU, Narvekar PV, Pratihary AK, Naik H, Shenoy DM, Jayakumar DA, Goepfert TJ, Patra PK, Al-Azri A (2010) The Arabian Sea as a high-nutrient, low-chlorophyll region during the late Southwest Monsoon. Biogeosciences 7:2091–2100

O'Reilly J E, Maritorena S, Siegel DA, O'Brien MC, Toole D, Mitchell BG, Kahru M, Chavez FP, Strutton P, Cota GF, and Hooker SB (2000), Ocean color chlorophyll a algorithms for SeaWiFS, OC2, and OC4: version 4. SeaWiFSpostlaunch calibration and validation analyses, Part, 3, pp.9–23

Patra PK, Kumar MD, Mahowald N, Sharma VVSS (2007) Atmospheric deposition and surface stratification as controls of contrasting chlorophyll abundance in the North Indian Ocean. J Geophys Res 112: C05029. https://doi.org/10.1029/2006JC003885

Pease PP, Tchakerian VP, Tindale NW (1998) Aerosols over the Arabian Sea: geochemistry and source areas for aeolian desert dust. J Arid Environ 39:477–496

Platt T, Sathyendranath S (1988) Oceanic primary production: estimation by remote sensing at local and regional scales. Science 241:1613–1620

Poll WH, Kulk G, Timmermans KR, Brussaard CPD, Woerd HJ, Kehoe MJ, Mojica KDA, Visser RJW, Rozema PD, Buma AGJ (2013) Phytoplankton chlorophyll a biomass, composition, and productivity along a temperature and stratification gradient in the northeast Atlantic Ocean. Biogeosciences 10:4227–4240

Prakash PJ, Stenchikov G, Kalenderski S, Osipov S, Bangalath H (2015) The impact of dust storms on the Arabian Peninsula and the Red Sea. Atmos Chem Phys 15(199–222):2015. https://doi.org/10.5194/acp-15-199-

Prakash PJ, Stenchikov G, Tao W, Yapici T, Warsama B, Engelbrecht JP (2016) Arabian Red Sea coastal soils as potential mineral dust sources. Atmos Chem Phys 16(18):11991–12004

Prakash S, Ramesh R (2007) Is the Arabian Sea getting more productive? Curr Sci 92(5):667–670

Prospero J, Nees RT, Uematsu M (1987) Deposition rate of particulate and dissolved aluminium derived from Saharan dust in precipitation at Miami, Florida. J Geophys Res *92*:14 723–14 731

Prospero JM, Ginoux P, Torres O, Nicholson SE, Gill TE (2002) Environmental characterization of global sources of atmospheric soil dust identified with the NIMBUS 7 TOMS absorbing aerosol product. Rev Geophys 40(1):1002. https://doi.org/10.1029/2000RG000095

Ramaswamy V, Muraleedharan PM, Babu CP (2017) Mid-troposphere transport of Middle-East dust over the Arabian Sea and its effect on rainwater composition and sensitive ecosystems over India. Sci Rep 7(1):13676

Remer LA, Tanre D, Kaufman YJ, Ichoku C, Mattoo S, Levy R, Chu DA, Holben B, Dubovik O, Smirnov A, Martins JV (2002) Validation of MODIS aerosol retrieval over ocean. Geophys Res Lett 29(12):8008

Rienecker MM, Suarez MJ, Gelaro R, Todling R, Bacmeister J, Liu E, Bosilovich MG, Schubert SD, Takacs L, Kim GK, Bloom S, Chen J, Collins D, Conaty A, da Silva A, Gu W, Joiner J, Koster RD, Lucchesi R, Molod A, Owens T, Pawson S, Pegion P, Redder CR, Reichle R, Robertson FR, Ruddick AG, Sienkiewicz M, Woollen J (2011) MERRA: NASA's modern-era retrospective analysis for research and applications. J Clim 24(14):3624–3648. https://doi.org/10.1175/JCLI-D-11-00015.1

Sarthou G, Baker AR, Blain S, Achterberg EP, Boye M, Bowie AR, Croot P, Laan P, Baar HJW, Jickells TD, Worsfold PJ (2003) Atmospheric iron deposition and sea-surface dissolved iron concentrations in the east Atlantic Ocean. Deep-Sea Res I Oceanogr Res Pap 50:1339–1352. https://doi.org/10.1016/S0967-0637(03)00126-2

Shang S, Dong Q, Lee Z, Li Y, Xie Y, Behrenfeld M (2011) MODIS observed phytoplankton dynamics in the Taiwan Strait: an absorption-based analysis. Biogeosciences. 8:841–850. https://doi.org/10.5194/bg-8-841-2011

Srinivas B, Sarin MM, Kumar A (2011) Impact of anthropogenic sources on aerosol iron solubility over the Bay of Bengal and the Arabian Sea. Biogeochem 110(1–3):257–268. https://doi.org/10.1007/s10533-011-9680-1

Srivastava AK, Soni VK, Singh S, Kanawade VP, Singh N, Tiwari S, Attri SD (2014) An early South Asian dust storm during March 2012 and its impacts on Indian Himalayan foothills: a case study. Sci Total Environ 493:526–534

Singh S, Beegum SN (2013) Direct radiative effects of an unseasonal dust storm at a western Indo Gangetic Plain station Delhi in ultraviolet, shortwave, and longwave regions. Geophys Res Lett 40:2444–2449. https://doi.org/10.1002/grl.50496

Singh RP, Prasad AK, Kayetha VK, Kafatos M (2008) Enhancement of oceanic parameters associated with dust storms using satellite data. J Geophys Res 113:C11008. https://doi.org/10.1029/2008JC004815

Smitha A, Joseph KA, Jayaram C, Balchand AN (2014) Upwelling in the southeastern Arabian Sea as evidenced by Ekman mass transport using wind observations from OCEANSAT–II Scatterometer. Ind J Geo-Mar Sci 43(1):111–116

Sunda WG, Hunstsman SA (1997) Interrelated influence of iron; light cell size on marine phytoplankton growth. Nature 390:389–392

Takahashi Y, Higashi M, Furukawa T, Mitsunobu S (2011) Change of iron species and iron solubility in Asian dust during the long-range transport from western China to Japan. Atmos Chem Phys 11:11237–11252. https://doi.org/10.5194/acp-11-11237-2011

Tan S-C, Shi G-Y, Shi J-H, Gao H-W, Yao X (2011) Correlation of Asian dust with chlorophyll and primary productivity in the coastal seas of China during the period from 1998 to 2008. J Geophys Res 116:G02029. https://doi.org/10.1029/2010JG001456

Tang D, Kawamura H, Luis AJ (2002) Short-term variability of phytoplankton blooms associated with a cold eddy in the northwestern Arabian Sea. Remote Sens Environ 81:82–89

Twomey S (1977) The influence of pollution on the shortwave albedo of clouds. J Atmos Sci 34:1149–1152

Uno I, Harada K, Satake S, Hara Y, Wang Z (2005) Meteorological characteristics and dust distribution of the Tarim Basin simulated by the nesting RAMS/CFORS dust model. J Meteorol Soc Jpn 83A:219–239

Volpe G, Banzon VF, Evans RH, Santoleri R, Mariano AJ, Sciarra R (2009) Satellite observations of the impact of dust in a low-nutrient, lowchlorophyll region: fertilization or artifact? Glob Biogeochem Cycles 23:1–14. https://doi.org/10.1029/2008GB003216

Vahtera E, Laanemets J, Pavelson J, Huttunen M, Kononen K (2005) Effect of upwelling on the pelagic environment and bloom-forming cyanobacteria in the western Gulf of Finland, Baltic Sea. J Mar Syst 58:67–82. https://doi.org/10.1016/j.jmarsys.2005.07.001

Vincent J, Laurent B, Losno R, Bon Nguyen E, Roullet P, Sauvage S et al (2016) Variability of mineral dust deposition in the western Mediterranean basin and south-east of France. Atmos Chem Phys 16(14):8749–8766

Wang SH, Hsu C, Tsay SC, Lin NH, Sayer AM, Huang SJ, William KML (2012) Can Asian dust trigger phytoplankton blooms in the oligotrophic northern South China Sea? Geophys Res Lett 39:L05811. https://doi.org/10.1029/2011GL050415

Wells ML (2003) The level of iron enrichment required to initiate diatom blooms in HNLC waters. Mar Chem 82:101–114

Wiggert JD, Hood RR, Banse K, Kindle JC (2005) Monsoon-driven biogeochemical processes in the Arabian Sea. Prog Oceanogr 65(2–4):176–213

Zhang GJ, McPhaden MJ (1995) The relationship between sea surface temperature and latent heat flux in the equatorial Pacific. J Clim 8(3):589–605

Zhu A, Ramanathan V, Li F, Kim D (2007) Dust plumes over the Pacific, Indian, and Atlantic oceans: climatology and radiative impact. J Geophys Res 112:D16208. https://doi.org/10.1029/2007JD008427